

NUMERICAL STUDY OF THE EFFECTS OF PROSTHESIS FOOT ASYMMETRY ON ENERGY CHARACTERS AND ROLL-OVER CHARACTERISTICS

MEIJIAO JIANG, JUNXIA ZHANG

College of Mechanical Engineering, Tianjin University of Science and Technology, Tianjin, China

correspondence author Junxia Zhang, e-mail: zjx@tust.edu.cn

There is limited research available on the effect of asymmetric structure on the performance of the prosthesis. In this paper, 12 sets of prosthetic feet with asymmetric structures were developed using a planar polar coordinate system. The effect of asymmetry on the prosthesis performance was investigated. The prosthetic feet with asymmetric structures were modeled in a gradient manner within a polar coordinate system. A finite element (FE) model of the prosthetic walking process was formulated, and dynamic simulations were conducted to simulate the loading of the prosthesis during the support phase. Evaluation indices such as energy characteristics, contact pressure and roll-over shape were selected to investigate the effects of the asymmetric structure. The results indicate that θ_1 and θ_3 asymmetry significantly affects strain energy density. Moreover, incorporating heel asymmetry proves to be more advantageous in reducing contact pressure of the prosthesis during the middle stance moment. The optimal parameters for asymmetric prostheses are determined based on these findings.

Keywords: biometric prosthetic foot, carbon fiber epoxy composites, roll-over shape, energy store and return character

1. Introduction

Proper amputee prosthetic component selection is critical in the improvement of the amputee care (Fridman *et al.*, 2003). Asymmetrically shaped prostheses were designed to improve patients' rehabilitation and quality of life. Preliminary studies were conducted on an asymmetrically shaped keel (Allard *et al.*, 1995) in the prosthetic foot design, and the results indicated that the asymmetrically shaped keel was more active in storing energy and improving amputee gait (Handzic, 2014) compared with a completely symmetrical one. However, the effect of asymmetric design of the prosthetic foot on user gait performance is unclear. There are three main types of methods for studying prostheses: theoretical calculations, testing of mechanical properties of prostheses and amputation gait analysis. The theoretical analysis method is primarily employed to calculate the angular stiffness of the forefoot and hindfoot (Adamczyk and Kuo, 2013). Calculated was mechanical efficiency during gait in adults with transtibial amputation (Prince *et al.*, 1998), and determined energy stored, dissipated and recovered in different ankle-foot prostheses (Prince *et al.*, 1994). Additionally, models of rigid segments of the prosthetic foot were developed (Fey *et al.*, 2013), and FE models provided to anticipate mechanical reactions to forces, moments and displacements (Tryggvason *et al.*, 2020). Furthermore, the finite element approach was used for dynamic simulation of prosthetic walking (Jang *et al.*, 2001).

Mechanical tests provide a valuable means to examine prosthetics, including forefoot and hindfoot stiffness, prosthetic energy storage characteristics and dynamic walking characteristics. For instance, Adamczyk *et al.*, (2013) used the linear compression method to measure angular

stiffness, whereas Adamczyk *et al.* (2017) adjusted stiffness of the forefoot and hindfoot components. They subsequently computed energy return of the prosthesis and assessed sensitivity of these variables to changes in component stiffness. Fey *et al.* (2011) conducted a comprehensive biomechanical investigation to evaluate the influence of foot stiffness on the prosthetic energy storage, energy return and mechanical efficiency during amputee walking. They incorporated forward dynamics models of amputee walking to further explore the impact of altered prosthetic foot stiffness on muscle and foot functions.

Gait analysis is used to study various parameters of amputee walking such as energy expenditure, gait asymmetry and prosthetic deformation. Gait characteristics under various types of walking conditions such as horizontal ground, ramps, self-selected and varying travel speeds are studied for their effects on gait, and dynamic joint stiffness is analyzed (Ármannsdóttir *et al.*, 2021). Among them, several specific gait moments such as heel strike, middle stand and toe-off are focused in (Adamczyk *et al.*, 2017). In previous studies, stiffness, energy, gait parameters and roll-over shape were the most commonly used prosthetic performance indicators (De Asha *et al.*, 2013; Adamczyk *et al.*, 2013; Hansen *et al.*, 2004a,n; Hansen and Childress, 2005).

The primary objective of this study is to examine the effect of asymmetric structure on the performance of prostheses. Addressing the limitations of prior research, this paper adopts a polar coordinate system to describe the location and degree of asymmetry of prostheses, thus filling the gap in quantitative investigations of structural asymmetry. The asymmetric foot model was established based on a commercially available carbon fiber ESAR foot (Össur Vari-flex®). Gait characteristics during the support phase of transtibial amputees were explored using a dynamic walking model. The asymmetric design of the prosthetic foot was investigated. Notably, this research presents an innovative application of contact pressure as an index for studying the effects of prosthetic asymmetry. The prosthetic model was derived from the Flex-Foot® Variflex® architecture and was studied both analytically and quantitatively using curved elements analysis as well as the Castigliano theorem (Hansen *et al.*, 2000).

2. Materials and methods

2.1. FE model

The transtibial prosthesis design model is based on the Össur Vari-flex® architecture (long $l = 241.523$ mm, category 5). The prosthesis is made up of two carbon fiber (CF) composite leaf springs: one for the keel and one for the heel (see Fig. 1a). Both the keel and heel were made of laminates with the stack sequence $[\pm 45/0_n]_s$ as shown in Fig. 1b, with 45° cross-ply layers on top and bottom, n is the 0° fiber layer number which is determined according to the prostheses thickness H , s indicates symmetrical plied layers. The value of n can be obtained from the following equation

$$H = h(2 + n)2 \quad (2.1)$$

where h is the thickness of the fiber layer.

The carbon blades are represented as flexible surface bodies. Each layer of the blades has its layer thickness, material characteristics, and fiber angle in the FE model. The model is created using ABAQUS.

In this work, a high strength carbon/epoxy prepreg (T300) was used. Its material properties are $E_{11} = 132$ GPa, $E_{22} = E_{33} = 10.3$ GPa, $G_{12} = 6.5$ GPa, $G_{13} = 6.5$ GPa, $G_{23} = 3.91$ GPa, $\nu_{12} = 0.25$, $\nu_{13} = 0.25$, $\nu_{23} = 0.38$ and $\rho = 1570$ kg/m³.

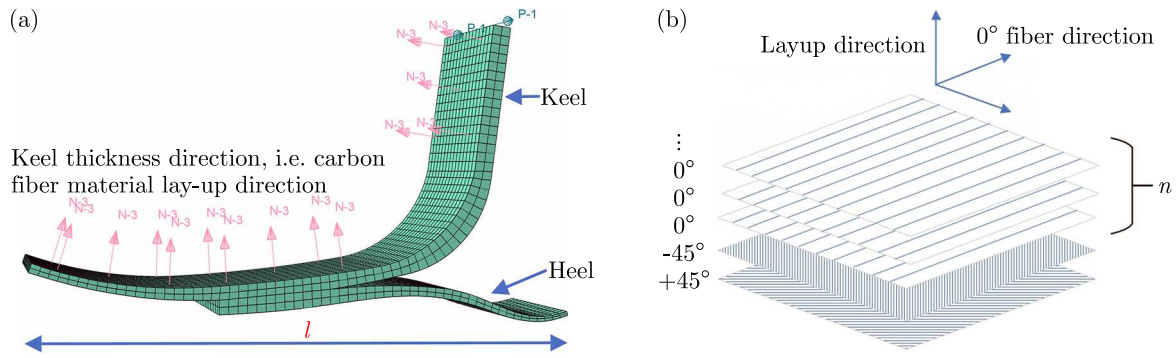


Fig. 1. (a) FE model of the prosthetic foot and (b) CF composite layer

2.2. Asymmetric prosthetic foot model

A planar polar coordinate system was established by taking the horizontal top view section of the prosthetic foot device. As shown in Fig. 2, l is length and w is width of the prosthesis. ‘Toe’ shows the toe direction, and ‘Heel’ is the position of the heel. Taking the geometric center of the insole as the origin of the polar coordinate system, denoted by O , ρ and θ are used to describe any point within the polar coordinates. Creating an asymmetric fillet at the left front position shown in Fig. 2, the radius of the fillet is denoted by r . The polar coordinates of this position are: $\rho = \sqrt{l^2 + w^2}/2 = \tan^{-1} w/l$, see Fig. 2.

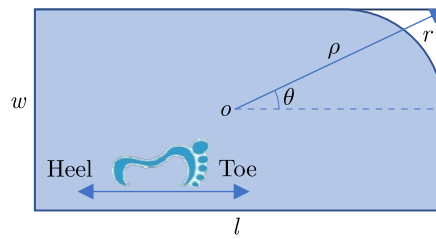


Fig. 2. Coordinate system of the asymmetric model

Fillets of different radii were created at each of the four corners of the prosthesis to create asymmetric models. The variables ρ , θ and r were used to describe the location and size of the asymmetric fillet (see Table 1). A total of twelve asymmetric prosthesis models were created.

Table 1. Asymmetric model fillet locations

ρ [mm]	θ [rad]	R_1 [mm]	R_2 [mm]	R_3 [mm]
$\rho = \sqrt{l^2 + w^2}/2$	$\theta_1 = \tan^{-1} w/l$	0	30	50
$\rho = \sqrt{l^2 + w^2}/2$	$\theta_2 = (\pi/2) + \tan^{-1} w/l$	0	20	30
$\rho = \sqrt{l^2 + w^2}/2$	$\theta_3 = \pi + \tan^{-1} w/l$	0	20	30
$\rho = \sqrt{l^2 + w^2}/2$	$\theta_4 = (3\pi/2) + \tan^{-1} w/l$	0	30	50

θ_1 and θ_4 are located at the front end of the keel placed on the inner and outer sides of the prosthetic foot, respectively. θ_2 and θ_3 are located at the back end of the keel, inside and outside.

2.3. Roll-over simulation

The prosthetic foot, loading frame and rotating platform are created for dynamic walking simulation according to ISO/TS 16955 (2016). The simulation shows results for a full roll-over

task of the prosthetic foot. One simulation cycle consists of the dynamic walking stance phase of a single gait step. The loading frame and the rotating platform were constructed as rigid bodies. A rigid beam is used to connect the fixed ankle of the foot to the loading frame, and rough contact without sliding is defined between the prosthetic foot and the surface of the rotating platform. The assembly model is shown in Fig. 3c. Transient structural analysis is carried out for the FE model of the foot. Figure 3a shows the simulation load-time curve according to ISO/TS 16955 (2016). The total time is a stance phase (0.6 s) of a standard gait cycle (1 s), and this load represents the ground reaction force of the stance phase of the amputation gait. Figure 3b shows the angle-time curve according to ISO/TS 16955 (2016). The loading frame is applied to simulate the amputee walking with a prosthesis in the right-side limb. The movement freedom of the top point *A* of the loading frame is equal to zero in the transverse plane, and the load Fig. 3a is applied to the top point of the loading frame, as shown in Fig. 3c. The rotating platform is assembled at a distance of 700 mm from the top point of the loading frame. The rotating platform is used to simulate the ground, where the platform rotates around point *B*. In the ISO standard, the ankle joint angle during walking is converted into ground rotation. During the support phase, the foot moves downward while the platform rotates, and it is pushed by point *A*. The ankle joint angle of the support phase is achieved by rotating the platform around point *B*. This can be seen in Fig. 3c, where the ankle angle is translated into rotation of the rotating platform around point *B*, and the load (Fig. 3b) is applied to the outside point *B* of the rotating platform to drive the rotation of the rotating platform to simulate the support phase in the amputation gait.

Taking three typical moments at $t_1 = 10$ ms, $t_2 = 300$ ms and $t_3 = 600$ ms as ‘heel-strike’, ‘middle-stance’ and ‘toe-off’ positions of the prosthesis, the loading frame and the tilted rotating platform as well as the corresponding stress and deformations of the prosthesis are shown in Figs. 3d, 3e, 3f.

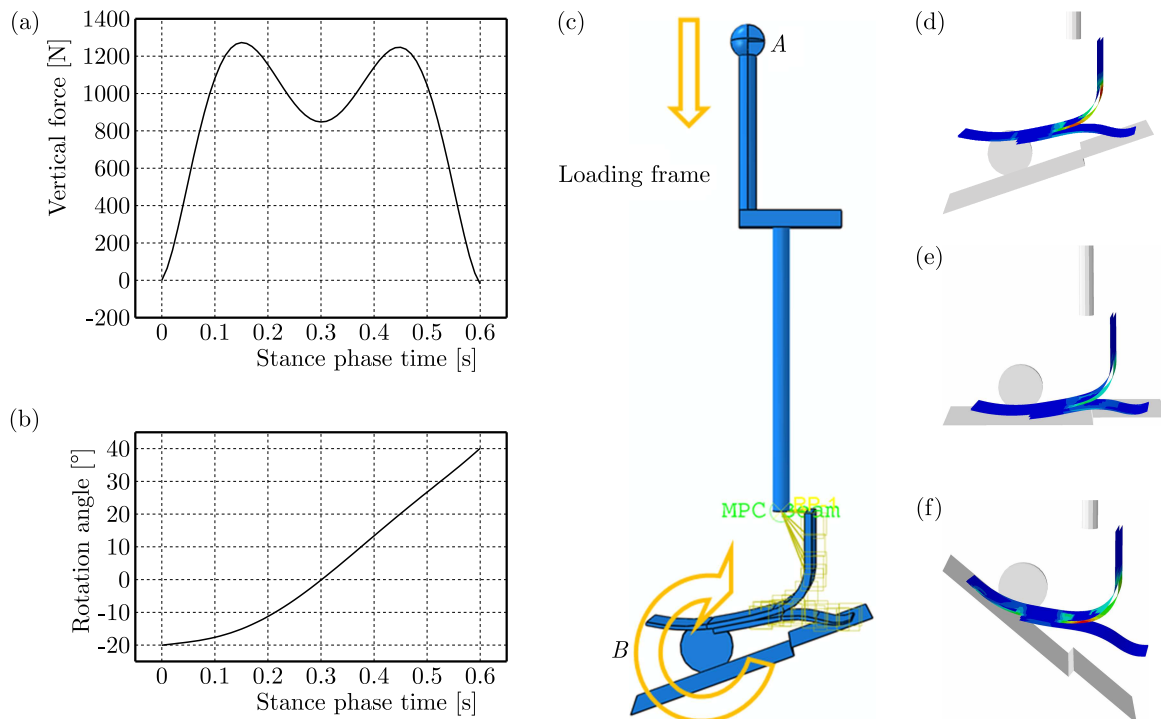


Fig. 3. Simulation process and the boundary condition diagram: (a) vertical force on the ball joint according to ISO/TS 16955, (b) rotation of tilt-table, as functions of the stance phase time, (c) boundary condition of full model transient simulation of ISO 16955 test procedure for a 600 ms loop, (d) showing stress at early heel-strike, at 10 ms, (e) mid-stance, at 300 ms, (f) toe-off at 600 ms

Twelve asymmetric prosthetic foot models were established according to the parameters ρ , θ and r in Table 1. The stance phase dynamic walking simulation was carried out for all the prosthetic foot models.

The strain energy, strain energy density, contact pressure and roll-over shape were extracted from the roll-over simulation, and used to discuss the gait characteristics of the asymmetric prosthetic foot structure.

2.4. Validation of simulation models

The simulation model was validated using the roll-over shape test data of the same series of different types of the prosthetic foot. The roll-over shape is expressed by the simulated CoP, the CoP is extracted from the foot and rotating contact points during the support phase roll-over simulation. No coordinate transformation is required because the simulation is set up with ground platform rotation and the relative position of the simulated leg is fixed. The comparison between the test data and the simulation data is shown in Fig. 4. The x -direction is the length direction of the prosthesis, and Y indicates the compression displacement of the foot-ground contact point on the lower surface of the prosthesis at each instant of the support phase.

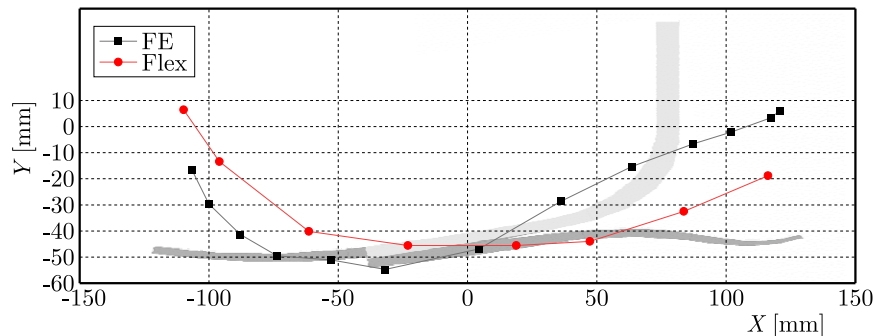


Fig. 4. Comparison of FE roll-over shape of the symmetrical-keel prosthetic foot and the test roll-over shape of the Össur Flexwalk prosthetic foot

As shown in the figure, the roll-over shape of the Flexwalk foot (Hansen *et al.*, 2000) is similar to the roll-over shape of the symmetric prosthetic foot simulation model, which proves that the simulation results are reliable.

3. Results and discussion

3.1. Strain energy density

The strain energy in the model is mainly stored in the heel part from the heel-strike to mid-stance period, and the keel part plays the main role in energy storage from the mid-stance to toe-off period. The following figure shows the heel strain energy density distribution at the heel-strike moment and the keel strain energy density cloud map at the toe-off moment. The strain energy density distribution for each asymmetric shape of the prosthesis are shown in Fig. 5, with the radius of the fillet in the first column, the polar angle in the first and fifth row to classify the asymmetric prosthesis model.

At the heel-strike moment, the strain energy is distributed in the middle and rear of the heel. The larger the asymmetric fillet, the larger the strain energy density distribution area is.

The keel component of the prosthetic foot is the main deformation component at the toe-off moment, and the strain energy is mainly distributed in the forefoot and midfoot. Forefoot

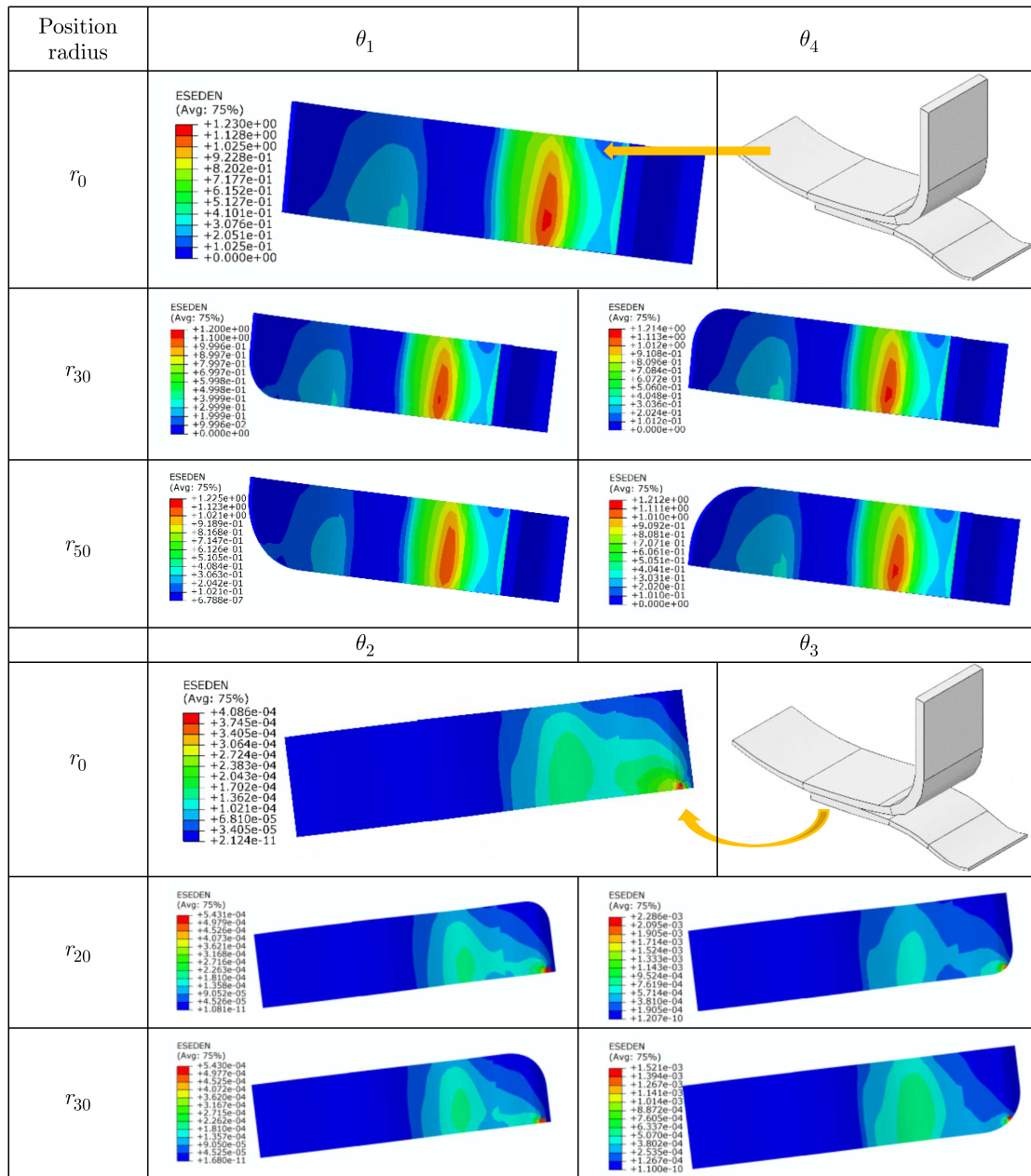


Fig. 5. Strain energy density distribution in the prosthetic foot model

asymmetry decreases the peak strain energy density, and forefoot asymmetry almost does not change the midfoot strain energy density distribution.

Figure 6 shows a comparison of the peak strain energy density for each prosthetic foot model. As shown in the figure, compared with the shape-symmetric prosthesis model, the peak strain energy density of the shape-asymmetric prosthesis model shows that the forefoot asymmetry slightly reduces the peak strain energy density. Compared with the heel symmetric prosthesis model, the heel asymmetry show an increase in the peak strain energy density, increase of θ_3 is significant, and the strain energy density of the r_{20} fillet shape asymmetric prosthetic model increases even more significantly.

As shown in Fig. 6, the strain energy density fluctuates considerably in magnitude due to the change of the asymmetry fillet radius. The θ_1 and θ_3 of the asymmetry shape prosthetic foot

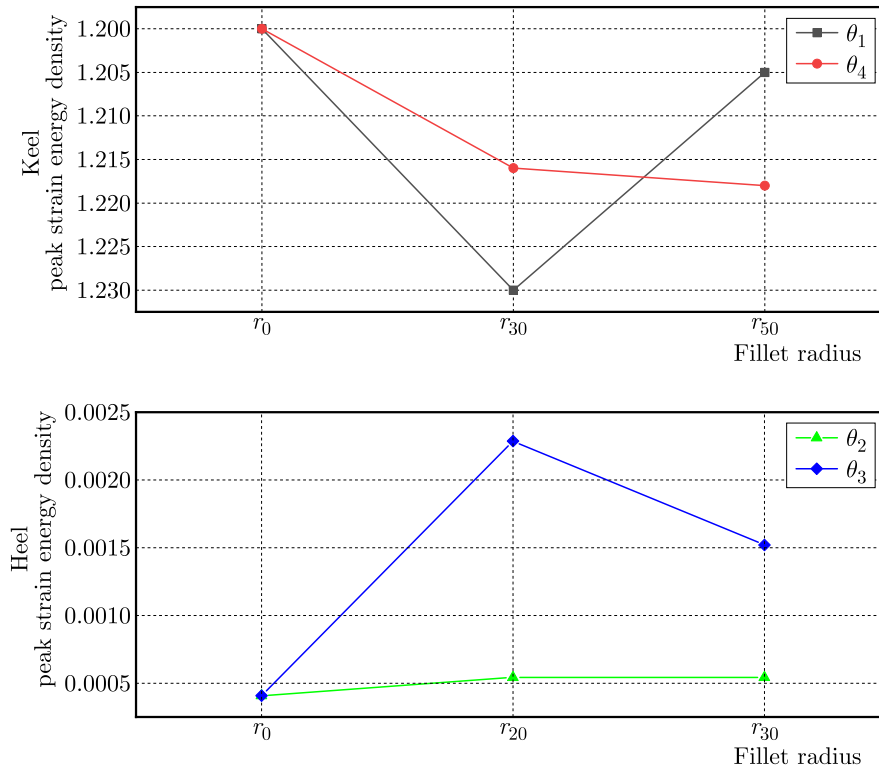


Fig. 6. Peak strain energy density of prosthetic foot models

have a relatively large effect on the strain energy density. The θ_2 and θ_4 of the asymmetry shape prosthetic foot have the least effect on the strain energy density.

3.2. Contact pressure

A comparison of the contact pressure between the symmetric and asymmetric shape prosthetic foot at the three characteristic moments of the support phase is shown in Fig. 7.

Comparing the contact pressure of the four groups of prosthetic feet, one can observe that the contact pressure of the θ_3 asymmetric prosthesis at the heel-strike is significantly higher than that of the symmetric prosthesis (Fig. 7 θ_3), and the contact pressure of the θ_1 and θ_4 asymmetric prosthesis at the toe-off is higher than that of the symmetric prosthesis (Fig. 7 θ_1 , Fig. 7 θ_4). The θ_1 and θ_4 group of the prosthetic foot have an asymmetric shape in the keel front, i.e. toe shape asymmetric model, and the contact pressure of the asymmetric prosthetic at the toe-off for both θ_1 and θ_4 groups is higher than that of the symmetric model at the toe-off moment. At the two aforementioned contact transients, the contact area is inversely proportional to the material elastic modulus, inversely proportional to the prosthesis thickness, and proportionate to the prosthesis horizontal projected area (Fig. 2). Due to the fact that we used the same elastic materials and the thickness in the simulation and that only the horizontal projection area of the prosthesis differed between the symmetric and asymmetric models, the horizontal projection area (asymmetric parameters) of the prosthesis is regarded as the primary factor influencing the contact area. According to the correspondence between the pressure and contact area, the magnitude of pressure p is inversely proportional to the contact area s for the same load f

$$p = \frac{f}{s} \quad (3.1)$$

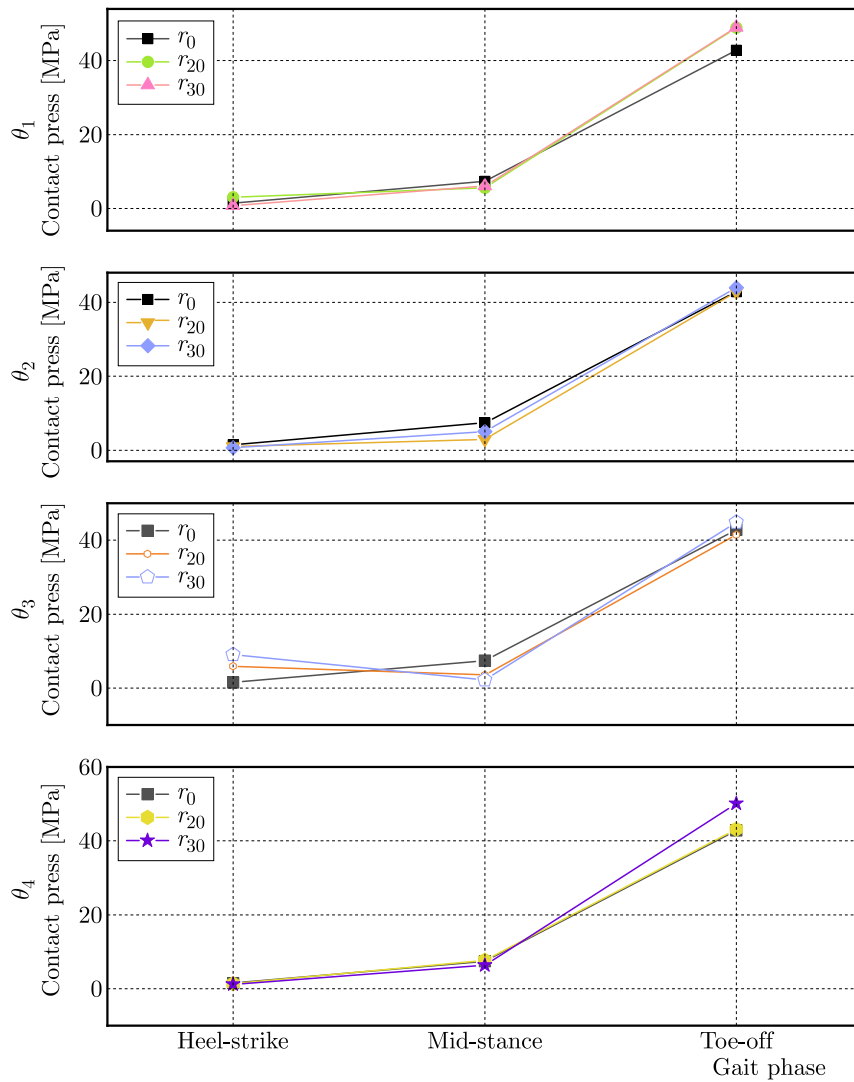


Fig. 7. Contact press at the heel-strike, mid-stance and toe-off moments

This phenomenon is because the force area of the asymmetric model is smaller than that of the symmetric model, which again proves the reliability of the analytical results.

Specifically analyzing the contact pressure at each moment, an interesting phenomenon is worth noting. At the moment of heel-strike, with the same heel asymmetry, the contact pressures of the θ_2 asymmetric model are lower than those of the 0-fillet symmetric model, in contrast to the phenomenon that the contact pressure of the asymmetric model of the θ_3 group is significantly higher than that of the 0-fillet symmetric model. The reason for this phenomenon may be that the inner asymmetric shape prosthetic model has a smaller contact area and lower model stiffness, but the impact reaction force is applied for a longer term than that of the symmetric model. The results indicate that the θ_2 asymmetry is beneficial to reduction of the heel-strike contact pressure. The asymmetry increases, and the contact pressure decreases subsequently. The θ_3 asymmetry has a negative effect on the contact pressure, the larger the asymmetry, the greater the contact pressure.

The contact pressure of θ_1 , θ_2 , θ_3 and θ_4 groups of asymmetric prosthesis models at the middle stance moment is smaller than that of the symmetric prosthesis models at that moment, which may be related to the decreased mass of the asymmetric prosthesis models compared with the symmetric prosthetic foot models. It indicates that the shape asymmetry can reduce the

contact pressure at the middle stance moment of the prosthesis; however, the contact pressure of the θ_2 and θ_3 asymmetric models is smaller than that of θ_1 and θ_4 asymmetric models, which indicates that the contact pressure at the middle stance moment is more influenced by the heel leaf, and this phenomenon is related to the location characteristics of the heel component of the prosthesis. The above results indicate that heel asymmetry is more beneficial to reduction of the contact pressure of the prosthesis at the middle stance moment compared to keel asymmetry.

3.3. Strain energy

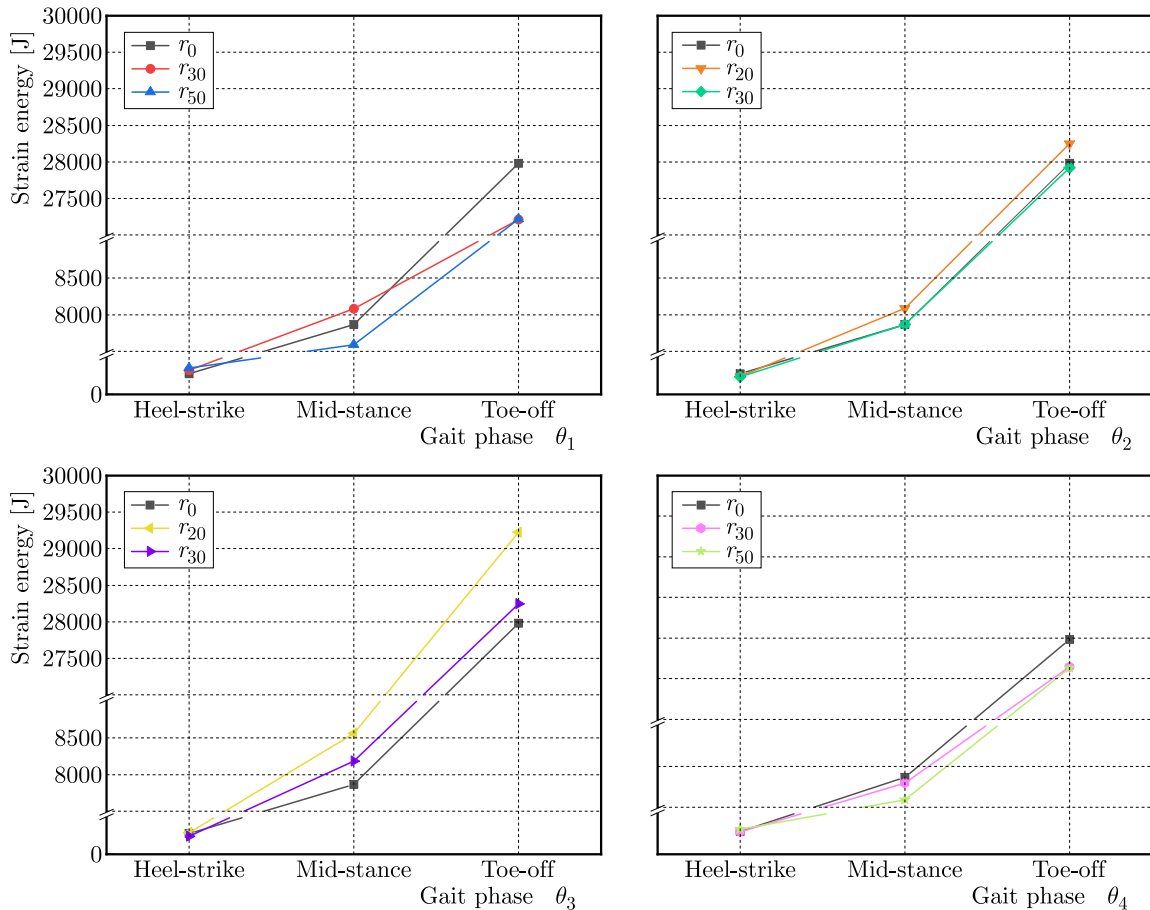


Fig. 8. The strain energy of each prosthetic foot

The strain energy of each prosthesis model at the three typical moments is shown in Fig. 8. The models are divided into θ_1 , θ_2 , θ_3 and θ_4 four categories according to the location of the shape asymmetry, and each of the three lines in each subgraph represents the size of an asymmetric fillet. The typical moments are heel-strike, middle stance and toe-off gait events.

The strain energy of the asymmetric prosthesis model at position θ_1 and θ_4 is smaller than that of the symmetric prosthesis model at the moment of toe-off. θ_1 is smaller, which indicates that the shape asymmetry at position θ_1 has the greatest negative impact on the strain energy, and the shape asymmetry at position θ_4 has a relatively small negative impact it. The strain energy of the prosthesis decreases as the asymmetry increases, but the correlation is not sensitive. The θ_2 and θ_3 asymmetries at positions θ_2 and θ_3 increase the strain energy, asymmetry at position θ_2 is more favorable to the strain energy, and the most favorable results are obtained when the radius of the fillet of the shape asymmetry at position θ_2 is 20 mm. The strain energy of the asymmetric fillet at 30 mm is similar to that of the symmetric prosthesis model. Asymmetry

at position θ_3 is partially favorable, but the results are uncertain and further studies should be conducted.

3.4. Strain energy calculations

It is necessary to analyze the energy generated in the foot module in order to determine the energy to be taken into the articulated area. This is achieved through the analysis of strain energy from the Castigliano theorem and the free body diagram of the foot module.

By employing the homogenization procedure, the keel structure is simplified into a cantilever model and a straightforward curved beam model (Fig. 9). The letters c and s stand for curved and straight (cantilever) beams. Axial, shear forces and bending moments combine to produce vertical deflection at the foot point of contact with the ground. When the radius-to-thickness ratio ($r = h$) is more than 10, the effects of the axial stress and shear are minimal (Boresi *et al.*, 1993).

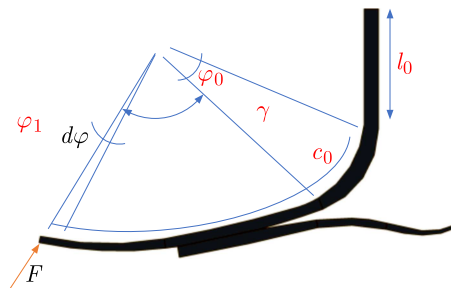


Fig. 9. Diagram of the toe-off working condition force

To determine beam deflection in this investigation, the strain energy that is exclusively attributable to bending is employed

$$\Delta = \frac{\partial U}{\partial F} \quad (3.2)$$

where F is the ground reaction force of the composite foot. The total strain energy U of the bionic prosthetic foot is expressed as follows

$$U = U_S + U_C \quad (3.3)$$

where the strain energy of the straight part U_S is expressed as follows

$$U_S = \int \frac{F_N^2}{2EA} dl + \int \frac{M_s^2}{2EI} dl \quad (3.4)$$

and the strain energy of the curved beam part is

$$U_C = \int \frac{F_S^2 \gamma}{2AG} d\varphi + \int \frac{F_N^2 \gamma}{2EA} d\varphi + \int \frac{A_m M_c^2}{2EA(\gamma A_m - A)} d\varphi \quad (3.5)$$

where E is longitudinal Young's modulus of the composite foot, A is the cross-sectional area, I is the moment of inertia, and dl is differential of the straight part length l_0 , γ is the curvature radius of curved parts c_0 , A_m is the distance from the center of the circumference of the curved beams, F_N is the axial stress, F_S is the shear stress, M_S and M_C represent the bending moments, and G is the shear modulus.

3.5. Roll-over shape

The roll-over shape of all prosthetic models is extracted as shown in Fig. 10, where the curve from the toe endpoint to $X = -75$ is defined as the toe region. $X = -75$ to $X = 0$ is defined as the forefoot region, and $X > 0$ is defined as the heel region according to the bionic structure. The X -axis direction is the length direction of the prosthesis, the heel is in the positive direction

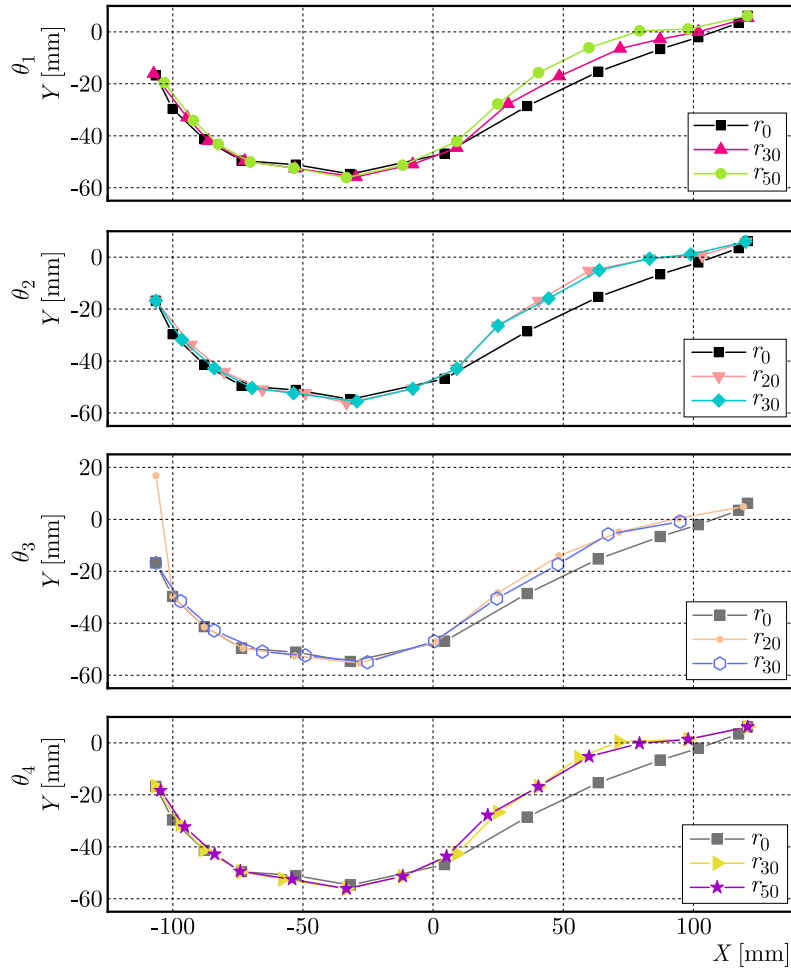


Fig. 10. The roll-over shape of the asymmetric prosthetic foot model compared with the roll-over shape of the symmetric prosthetic foot model. The upper subfigure shows the roll-over shape of the forefoot asymmetric prosthetic foot model compared with the symmetric model; the lower subfigure shows the roll-over shape of the heel asymmetric prosthetic foot model compared with the symmetric model

of the X -axis, the heel-strike corresponds to the right endpoint and is the starting point of the roll-over shape, the toe-off corresponds to the negative direction of the X -axis. The toe-off corresponds to the left endpoint of the curve and is defined as the endpoint of the roll-over shape.

The roll-over shape radius at the toe of the forefoot of the asymmetric prosthesis is reduced compared to that of the symmetric prosthesis, with the smallest roll-over shape radius at the toe of the 50 mm fillet prosthesis on the left side of the forefoot.

The radius of the roll-over shape at the toe of the forefoot of the asymmetric prosthesis is the smallest, and the radius of the roll-over shape is similar and slightly larger than that of the symmetric prosthesis.

The toe-off points of the four θ_1 , θ_2 , θ_3 and θ_4 asymmetric prosthetic feet models are compared with the toe-off points of the symmetric model prosthetic feet. Only the toe-off point

of the right heel 20 mm fillet asymmetric model is much higher than the toe-off point of the symmetric model of the prosthetic foot, and the toe-off points of the rest of the heel of the asymmetric model almost overlapped with those of the symmetric model.

The asymmetry of the heel results in a reduced roll-over shape radius of the toe compared to the symmetric prosthetic foot. Specifically, the roll-over shape radius of the toe exhibits a 20 mm fillet on the left side of the heel and a 30 mm fillet on the right side of the heel, overlapping with the roll-over shape of the symmetric model.

Furthermore, the roll-over shape radius at the forefoot of the heel of the asymmetric prosthetic foot is similar to, and slightly larger than, the roll-over shape radius at the forefoot of the symmetric prosthetic foot. The shape asymmetry reduces the stiffness of the prosthesis relative to that of the fully symmetric model, making the roll-over deformation of the asymmetric prosthetic foot model larger than that of the symmetric prosthetic foot model. Among them, the roll-over shapes of the asymmetric fillets at positions θ_1 and θ_3 are of interest. The results in Fig. 10 show that the asymmetry at positions θ_1 and θ_3 has a greater effect on the roll-over shape of the prosthesis, and the asymmetry at positions θ_2 and θ_4 has a less effect on the roll-over shape of the prosthesis.

4. Conclusions

The effect of asymmetric shape on prosthetic performance has been innovatively studied, and the polar coordinate method has been innovatively used to describe the asymmetric position and degree of asymmetry. The amputee gait process of the support phase of the prosthetic foot was studied using the Össur prosthetic foot as the base model, and the gait behavior of the prosthetic foot in the support phase was investigated using dynamic walking numerical analysis. The design parameters of the asymmetric prosthetic foot were investigated using energy characteristics, contact pressure and roll-over shape of the support phase as performance indexes.

The θ_1 and θ_3 asymmetry shape prosthetic foot has a relatively large effect on the strain energy density. The θ_2 and θ_4 asymmetry shape prosthetic foot has the least effect on the strain energy density.

The heel asymmetry is more beneficial to reduction of the contact pressure of the prosthesis at the middle stance moment compared to the keel asymmetry.

The shape asymmetry at position θ_1 has a negative impact on the strain energy of the prosthesis, and the shape asymmetry at position θ_4 has a relatively small negative impact on the strain energy of the prosthesis. The most favorable results were obtained for the radius of the fillet of the shape asymmetry at position θ_2 was 20 mm. Asymmetry at position θ_3 was partially favorable.

The asymmetry at position θ_1 and θ_3 has a greater effect on the roll-over shape of the prosthesis, and the asymmetry at position θ_2 and θ_4 has a less effect on the roll-over shape of the prosthesis.

In summary, the optimal asymmetric prosthesis parameters are derived in this paper as shown in Table 2.

Table 2. Asymmetric prosthetic model

ρ [mm]	θ [rad]	R_1 [mm]
$\rho = \sqrt{l^2 + w^2}/2$	$\theta_1 = \tan^{-1} w/l$	0
$\rho = \sqrt{l^2 + w^2}/2$	$\theta_2 = (\pi/2)/2 + \tan^{-1} w/l$	20
$\rho = \sqrt{l^2 + w^2}/2$	$\theta_3 = \pi + \tan^{-1} w/l$	30
$\rho = \sqrt{l^2 + w^2}/2$	$\theta_4 = (3\pi/2) + \tan^{-1} w/l$	50

Acknowledgment

This work was supported by Tianjin Postgraduate Research Innovation Project (grant No. 2020YJSB065 and 2019YJSB014), Tianjin Science and Technology Plan Project (grant No. 20JCYBJC01430).

References

1. ADAMCZYK P.G., KUO A.D., 2013a, Mechanical and energetic consequences of rolling foot shape in human walking, *Journal of Experimental Biology*, **216**, 14, 2722-2731
2. ADAMCZYK P.G., ROLAND M., HAHN M.E., 2013b, Novel method to evaluate angular stiffness of prosthetic feet from linear compression tests, *Journal of Biomechanical Engineering*, **135**, 10, 104502-104505
3. ADAMCZYK P.G., ROLAND M., HAHN M.E., 2017, Sensitivity of biomechanical outcomes to independent variations of hindfoot and forefoot stiffness in foot prostheses, *Human Movement Science*, **54**, 154-171
4. ALLARD P., TRUDEAU F., PRINCE F., DANSEREAU J., LABELLE H., DUHAIME M., 1995, Modelling and gait evaluation of asymmetrical-keel foot prosthesis, *Medical and Biological Engineering and Computing*, **33**, 1, 2-7
5. ÁRMANNSDÓTTIR A.L., LECOMTE C., BRYNJÓLFSSON S., BRIEM K., 2021, Task dependent changes in mechanical and biomechanical measures result from manipulating stiffness settings in a prosthetic foot, *Clinical Biomechanics*, **89**, 105476
6. BORESI A.P., SCHMIDT R.J., SIDEBOTTOM O.M., 1993, *Advanced Mechanics of Materials*, New York: Wiley
7. DE ASHA A.R., JOHNSON L., MUNJAL R., KULKARNI J., BUCKLEY J.G., 2013, Attenuation of centre-of-pressure trajectory fluctuations under the prosthetic foot when using an articulating hydraulic ankle attachment compared to fixed attachment, *Clinical Biomechanics*, **28**, 2, 218-224
8. FEY N.P., KLUTE G.K., NEPTUNE R.R., 2011, The influence of energy storage and return foot stiffness on walking mechanics and muscle activity in below-knee amputees, *Clinical Biomechanics*, **26**, 10, 1025-1032
9. FEY N.P., KLUTE G.K., NEPTUNE R.R., 2013, Altering prosthetic foot stiffness influences foot and muscle function during below-knee amputee walking: a modeling and simulation analysis, *Journal of Biomechanics*, **46**, 4, 637-644
10. FRIDMAN A., ONA I., ISAKOV E., 2003, The influence of prosthetic foot alignment on trans-tibial amputee gait, *Prosthetics and Orthotics International*, **27**, 1, 17-22
11. HANDZIC I., 2014, *Analysis and Application of Passive Gait Rehabilitation Methods*, University of South Florida
12. HANSEN A.H., CHILDRESS D.S., 2005, Effects of adding weight to the torso on roll-over characteristics of walking, *Journal of Rehabilitation Research and Development*, **42**, 3
13. HANSEN A.H., CHILDRESS D.S., KNOX E.H., 2000, Prosthetic foot rollover shapes with implications for alignment of transtibial prostheses, *Prosthetics and Orthotics International*, **24**, 3, 205-215
14. HANSEN A.H., CHILDRESS D.S., KNOX E.H., 2004a, Roll-over shapes of human locomotor systems: effects of walking speed, *Clinical Biomechanics*, **19**, 4, 407-414
15. HANSEN A.H., CHILDRESS D.S., MIFF S.C., 2004b, Roll-over characteristics of human walking on inclined surfaces, *Human Movement Science*, **23**, 6, 807-821
16. ISO/TS 16955: 2016, Prosthetics – quantification of physical parameters of ankle foot devices and foot units

17. JANG T.S., LEE J.J., LEE D.H., YOON Y.S., 2001, Systematic methodology for the design of a flexible keel for energy-storing prosthetic feet, *Medical and Biological Engineering and Computing*, **39**, 1, 56-64
18. PRINCE F., WINTER D.A., SJONNENSEN G., POWELL C., WHEELDON R.K., 1998, Mechanical efficiency during gait of adults with transtibial amputation: a pilot study comparing the SACH, Seattle, and Golden-Ankle prosthetic feet, *Journal of Rehabilitation Research and Development*, **35**, 2, 177-185
19. PRINCE F., WINTER D.A., SJONNESEN G., WHEELDON R.K., 1994, A new technique for the calculation of the energy stored, dissipated, and recovered in different ankle-foot prostheses, *IEEE Transactions on Rehabilitation Engineering*, **2**, 4, 247-255
20. TRYGGVASON H., STARKER F., LECOMTE C., JONSDOTTIR F., 2020, Use of dynamic FEA for design modification and energy analysis of a variable stiffness prosthetic foot, *Applied Sciences*, **10**, 2, 650

Manuscript received February 16, 2023; accepted for print June 6, 2023